

NON-UNIFORM SPATIAL SAMPLING IN EEG SOURCE ANALYSIS

C.G. Bénar, J. Gotman

Montreal Neurological Institute, McGill University, Montréal, PQ, Canada

Abstract -We investigate in this paper the non-uniform sampling of EEG dipolar potentials and its impact on source analysis. We suppose some a priori knowledge on the approximate location of the dipole. We show that, in a noise-free situation, the electrode spacing needs to be around 3cm in the region of the dipole only, whereas it can drop to 8cm in remote regions.

Keywords - EEG source analysis, non-uniform sampling, potential on a sphere

I. INTRODUCTION

In electrophysiology, source reconstruction techniques can be used in order to find the sources of events observed on the electroencephalogram (EEG), such as evoked potentials or epileptic spikes. These methods make use of models of the head (e.g. 3 concentric spheres) and sources (e.g. current dipoles). Their aim is to find the set of sources that best explain the potentials measured at the level of the scalp. The choice of the number of recording points (electrodes) is essentially a problem of spatial sampling of the electrical potential at the head surface. Several authors ([1], [2], [3]) have studied this problem under the angle of Fourier analysis in order to find the minimum spatial frequency at which one should sample (Nyquist principle). This led them to the conclusion that one needs a large number of electrodes (more than 100) in order to avoid aliasing. It may however be very time-consuming to place such a large number of electrodes, which can be problematic - especially in a clinical setting. We address here the issue of a non-uniform sampling scheme, in which one would use a priori knowledge in order to put more electrodes (sampling points) in the regions where the potential has the higher spatial frequency content.

We studied non-uniform sampling of the potential of a dipole located close to the surface in a spherical model. We used the distortion approach of [4] in order to estimate the local bandwidth. We smoothed this function in order to take into account the uncertainty on dipole location that would exist in a real situation. We obtained a sampling scheme, and compared it with standard uniform (10/10 system) and non-uniform schemes using a dipole scan.

II. METHODOLOGY

A. Dipole potential

We used the classical 3-sphere model in order to simulate the potential of a dipolar source located 3mm under the brain surface [5] (Fig. 1). This configuration is representative of the

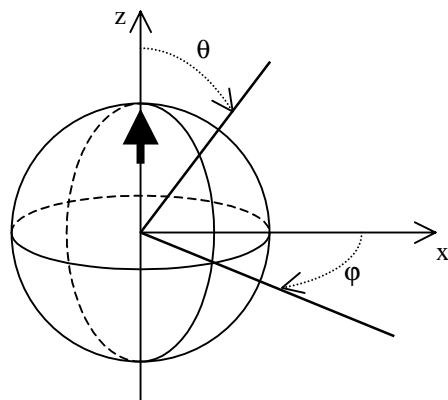


Fig.1: Coordinates (θ, ϕ) of a point on the surface of the outer sphere (dot) and schematic view of the dipole (arrow).

higher spatial frequency content one can get in EEG: the dipole is the most concentrated measurable source, and the "sharpness" of the potential increases with eccentricity. As the potential is invariant by rotation around the axis passing through the dipole, we will reduce the two-dimensional problem of sampling the potential $P(\theta, \phi)$ to the much simpler one-dimensional situation $\{P(\theta), \theta \in [-\pi, \pi]\}$.

B. Non-uniform sampling scheme

We used the approach in [4] that proposes to find - when possible - a nonlinear coordinate transformation $\theta' = \gamma(\theta)$ in order to map $P(\theta)$ onto a band-limited $h(\theta') = P(\gamma^{-1}(\theta'))$. We chose $h(\theta') = \cos(\theta')$, the simplest function that meets these requirements. In [4], the band-limited function is uniformly sampled at $\theta'_n, n = 0, \dots, N$, and a non-uniform sampling scheme is obtained at $\theta_n = \gamma^{-1}(\theta'_n)$ (Fig. 2).

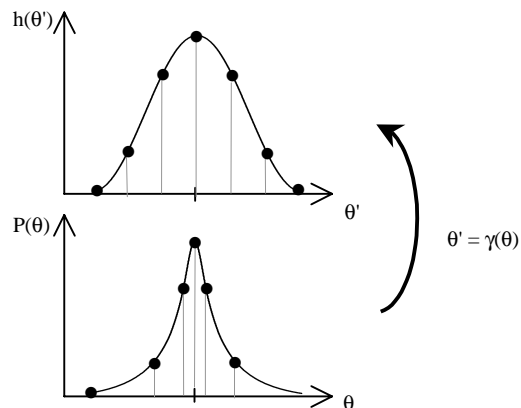


Fig. 2: Coordinate transformation between the band-limited function $h(\theta')$ (sampled uniformly), and the potential $P(\theta)$ (sampled non-uniformly).

If $h(\theta')$ is bounded in frequency by B_0 , then we can define for $P(\theta)$ the "local" bandwidth $B(\theta)$ as

$$B(\theta) = B_0 \partial\gamma/\partial\theta \quad (1)$$

In our case, $B_0 = 1/(2\pi R)$ cycles·cm⁻¹, with R head radius.

The mapping $\gamma(\theta)$ can be seen as a 'distortion' function that compresses the abscissa where the local bandwidth $B(\theta)$ is higher than B_0 and dilates it when $B(\theta)$ is smaller than B_0 . Thus, a higher rate of distortion indicates a higher local bandwidth. Once $B(\theta)$ is obtained, one can get the minimum local sampling rate $F_{\min}(\theta)$ as

$$F_{\min}(\theta) = 2 \cdot B(\theta) \quad (2)$$

In source analysis methods, one does not know by definition where the source lies. However, there is often some a priori knowledge of the region where the source should be, e.g. a fraction of a brain lobe. This region can be represented in our model by an angular interval, say $[-\theta_{\max}, \theta_{\max}]$. We chose to translate this interval of uncertainty by smoothing (i.e. convolving) the dipole spatial bandwidth with a gaussian filter $G(\theta)$ of FWHM $2 \cdot \theta_{\max}$:

$$B_{\text{smoothed}}(\theta) = G(\theta) * B(\theta) \quad (3)$$

In this study, $\theta_{\max} = \pi/8$ (the distance between two electrodes in the 10/10 system).

In the dipolar potential case, we were confronted with the fact that the frequency varies very rapidly with θ . This makes it especially difficult to define a sampling scheme that obeys (2), as the local bandwidth varies significantly from one sample to the next. We chose to start at $\theta_0 = 0$ - the center of symmetry of the potential - and take consecutive samples as:

$$\theta_{i+1} = 2 \cdot B_{\text{smoothed}}(\theta_i) \quad (4)$$

As $B_{\text{smoothed}}(\theta)$ decreases with $|\theta|$, (4) insured that the distance between a point at θ_i and any neighbor was no more than $2 \cdot B(\theta_i)$.

C. Comparison of sampling schemes

The different sampling schemes are summarized in Table I. For each scheme $\{\theta_i, i=1, \dots, n\}$ we calculated at each point (x, y) of a 10mm-spaced 2D grid the dipole that fits best the data $P(\theta_i)$ in a least-square sense.

TABLE I: SAMPLING SCHEMES

	Name	Minimum spacing (angle)	Maximum spacing (angle)	# points
1	10/10	36mm ($\pi/8$)	-	11
2	10/20	72mm ($\pi/4$)	-	5
3	Non-uniform	29mm	81mm	7

(Distances are given for a head radius of 92mm)

We measured the goodness of fit (g.o.f.) of the potential $P_{x,y}^{\text{fit}}$ by:

$$gof(x, z) = 1 - \frac{\sum_i [P(\theta_i) - P_{x,y}^{\text{fit}}(\theta_i)]^2}{\sum_i [P(\theta_i)]^2} \quad (5)$$

III. RESULTS

Figure 3 presents the normalized local bandwidth $B(\theta)/B_0$. It reaches a peak of approximately 10, which corresponds according to (2) to a minimum spacing of $1/F_{\min}(\theta) = 2\pi R / (2 \cdot 10) \approx 29\text{mm}$. Moreover, $B(\theta)/B_0$ decreases fast with $|\theta|$: it passes below 20% of the peak for $|\theta| \approx \pi/9$.

Figure 4 presents the different sampling schemes and the g.o.f. surfaces computed according to (5). One can interpret the surfaces in the following manner. At a given distance from the true dipole location, the smaller the g.o.f., the less likely will this point become a global maximum in a more realistic noisy situation. In other words, with a steeper surface, one would expect a smaller mean localization error.

We observe in Fig. 4 that the surface corresponding to the non-uniform scheme behaves similarly to that of the 10/10 scheme in the region of the dipole. At a distance, the behavior is more that of the 10/20, which is less critical because we are dealing with much smaller g.o.f. in these regions.

IV. DISCUSSION

We have found in our example that one needs a sampling period of approximately 3cm in the region of the dipole. This is in the range of values given in the literature, and close to the 10/10 spacing. However, in regions far away from the true dipole location, the sampling rate can drop to values of the order of those of the 10/20 system without a significant loss of source analysis performance, at least in a noise-free situation.

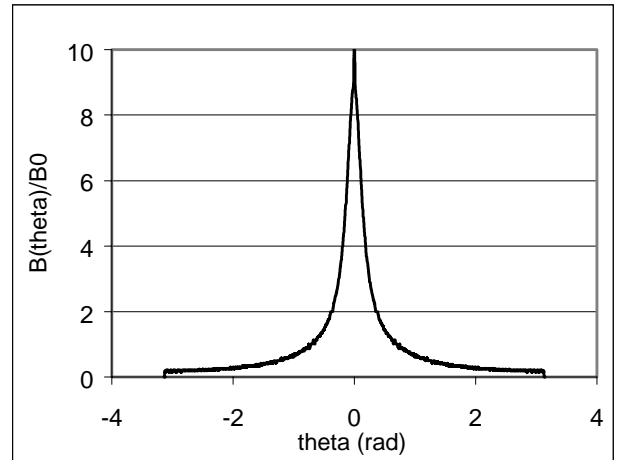


Fig. 3: Normalized local spatial frequency $B(\theta)/B_0$ for a radial dipole 3mm below the brain sphere.

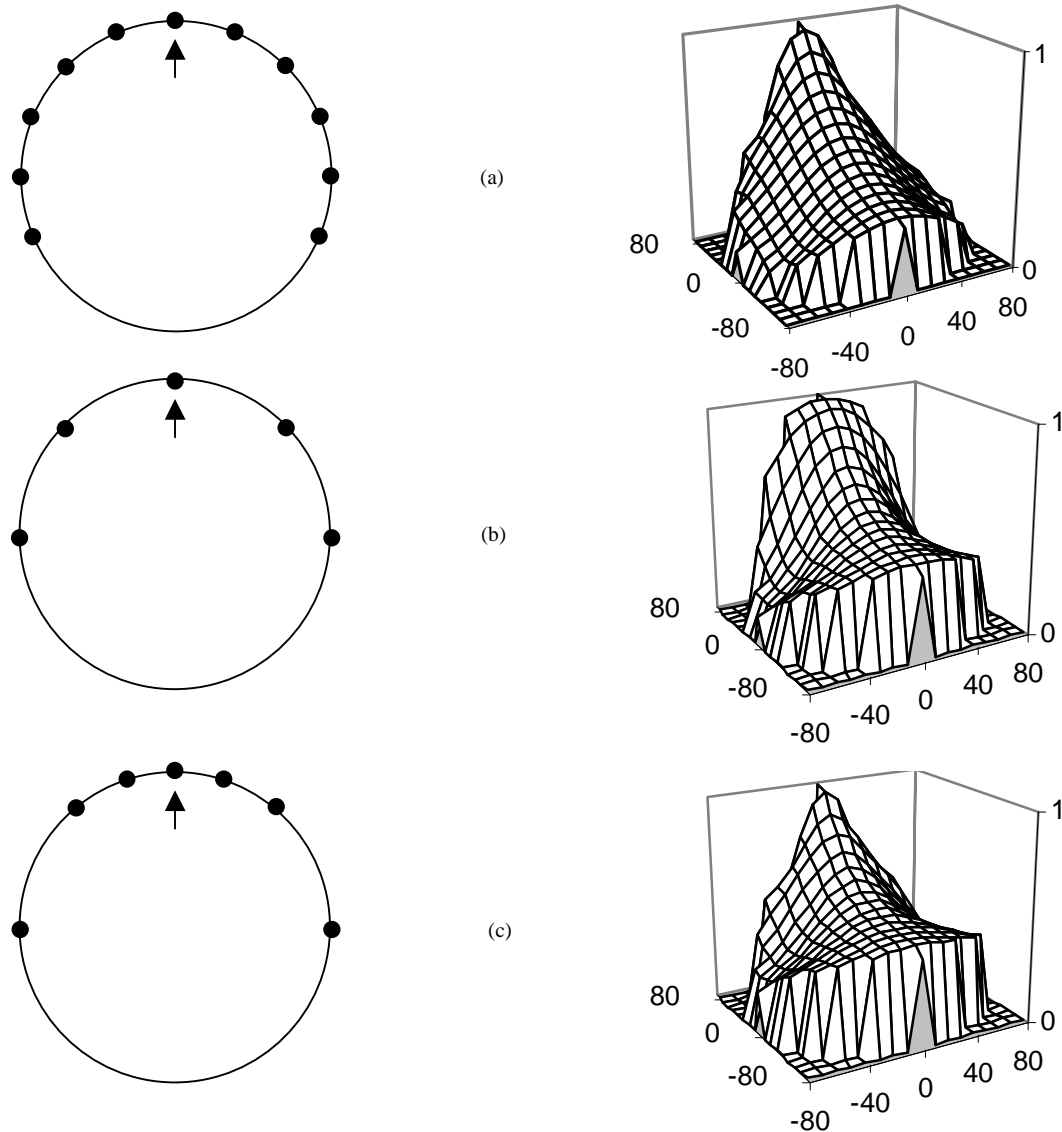


Fig. 4: The different sampling schemes with the original dipole location (left) and the corresponding g.o.f. surfaces (right): (a) 10/10, (b) 10/20, (c) non-uniform. Note how g.o.f. surfaces peak at the original dipole location.

V. CONCLUSION

We presented a method in order to construct an optimal sampling scheme of a dipolar field, based on non-uniform sampling theory and some *a priori* knowledge on dipole localization. This paper is set in the framework of dipole source analysis, but the method can be extended to more general spatial sampling problems.

REFERENCES

- [1] H. Holman, "Relation between depth and surface EEG", Thesis, Dept. of EE, report 200, Twente University of technology, 1979
- [2] A.S. Gevins, "Dynamic patterns in multiple lead data", in Event-related brain potentials: basic issues and applications, pp. 44-56, Oxford University Press, 1990
- [3] M. van Burik, G. Edlinger, G. Pfurtscheller, "Spatial mapping of ERD/ERS" in Event-related desynchronization, Handbook of Electroencephalography and Clinical Neurophysiology, revised series, Vol. 6, pp 107-118, 1999
- [4] J.J. Clark, M.R. Palmer, P.D. Lawrence, "A transformation method for the reconstruction of functions from nonuniformly spaced samples", IEEE Trans. Acoust., Speech, Sig. Proc., Vol. ASSP-33, No. 4, pp. 1151-1165, Oct. 1985
- [5] J.P. Ary, S.A. Klein, "Location of sources of evoked scalp potentials: corrections for skull and scalp thicknesses", IEEE Trans. Biomed. Eng., BME-28, No. 6, pp. 447-452, Jun. 1981